Quantum Electronics **50** (2) 136–140 (2020)

LASERS https://doi.org/10.1070/QEL17180

Tunable semiconductor laser with two acousto-optic tunable filters in its external cavity

L.N. Magdich, A.Yu. Chamorovskiy, V.R. Shidlovsky, M.V. Shramenko, S.D. Yakubovich

Abstract. **We report a laser with a linear external cavity containing a near-IR injection semiconductor optical amplifier as a gain element and two acousto-optic tunable filters (AOTFs) with quasi-collinear interaction of acoustic and light waves. At identical frequencies of RF signals that control the filters and ensure compensation for the Doppler frequency shift of light passing through the AOTFs, the steady-state laser emission linewidth can be reduced to about 25 MHz, which is almost three orders of magnitude smaller than that in the case of one filter (20 GHz). The position of the emission line, which remains narrow, slowly fluctuates within a spectral range about 3 GHz wide, which seems to be due to the large length of the external cavity and insufficient thermal stabilization of its components. This does not prevent us from obtaining light with a large coherence length. In emission wavelength sweep mode, the instantaneous emission linewidth increases with tuning rate, reaching 0.022 nm (8.8 GHz) at the highest tuning rate: 10^4 nm s^{-1}. In the case of automatic control over the output optical power at a level of 3 mW, the tuning range is 815–875 nm. Such instruments are of practical interest for optical coherence tomography, spectroscopy, optical metrology, and other application areas.**

Keywords: *tunable laser, semiconductor optical amplifier, acousto-optic filter, optical coherence tomography.*

1. Introduction

Semiconductor injection lasers capable of rapidly and very accurately tuning their emission wavelength are the most demanded in the current market for such instruments. The small size of modern optoelectronic components has enabled the advent of compact external laser cavity configurations. Involving various optoelectronic elements (volume diffraction gratings, acousto-optic elements, and electro-optical devices), such configurations allow a high wavelength tuning rate to be reached at a high wavelength reproduction accuracy. Owing to these advantages, such instruments are being increasingly widely used in various areas of science and technology, primarily in optical coherence tomography (OCT), including swept source (SS) and full field (FF) OCT systems; spectroscopy; optical sensors; etc.

There is currently great interest in acousto-optic tunable filters (AOTFs) as wavelength-selective elements capable of rapidly tuning the emission wavelength in a laser cavity, because they are compact, highly reliable and easy to control by an RF signal. The last is a key advantage of such instruments because it ensures high accuracy in setting and reproducing the emission wavelength in both a steady state and sweep mode. In this respect, they compare favourably to wavelength-selective elements with mechanically moving parts, which typically have low reliability, backlash and motion hysteresis.

Along with their obvious advantages, acousto-optic instruments have drawbacks. The main drawback of using them in an external laser cavity is the Doppler frequency shift of the optical frequency of the light passing through an AOTF [1], which impairs the performance of the laser, primarily increasing its emission bandwidth. The use of optical cavity configurations capable of compensating for this frequency shift is an effective approach for reducing the laser emission bandwidth.

This paper examines one possible external laser cavity configuration, similar to those described previously [2–4], which has two acousto-optic filters that compensate for the optical frequency shift in the AOTFs. The purpose of this study, which is a continuation of our previous work [5], is to develop an optical scheme of a laser rapidly tunable in a wide spectral range, suitable for practical implementation in the form of a compact instrument.

2. Optical scheme of the laser

Figure 1 shows the linear external cavity laser configuration used in this study. The gain element used was a two-pass bent active channel semiconductor optical amplifier (SOA) [6] based on a nanoheterostructure ensuring optical amplification in the spectral range 810–880 nm [7]. The SOA module, having input/output PANDA PM 850 polarisation-maintaining single-mode fibre (SMF) pigtails, was housed in a butterfly package containing a Peltier microcooler and thermistor, which ensured thermal stabilisation of the gain element. The output SOA facet, with a reflectivity of 20%, served as the external-cavity mirror. The other facet, facing the external cavity, had an anti-reflection coating. As a wavelength-selective element, we used a pair of quasi-collinear AOTFs with a transmission bandwidth near 0.2 nm in the spectral range indicated above. The filters were placed so that the Doppler

L.N. Magdich OJSC M.F. Stel'makh Polyus Research Institute, ul. Vvedenskogo 3/1, 117342 Moscow, Russia;
A.Yu. Chamorovskiy Superlum Diodes Ltd, Unit B3, Fota Point Enterprise Park, T45FC93 Carrigtwohill, Co Cork, Ireland;
V.R. Shidlovsky, M.V. Shramenko Opton Ltd., Mosfil'movskaya ul. 17B, 119330 Moscow, Russia;
S.D. Yakubovich Moscow Technological University (Moscow Institute of Radio Engineering, Electronics and Automation), prosp. Vernadskogo 78, 119454 Moscow, Russia;
e-mail: yakubovich@superlumdiodes.com

Received 5 November 2019; revision received 20 December 2019
Kvantovaya Elektronika **50** (2) 136–140 (2020)
Translated by O.M. Tsarev

shifts produced by them in the optical frequency compensated for each other. As the second mirror of the external cavity at the AOTF2 output, we used a dielectric broadband mirror with a near 100% reflectivity. The cavity length was about 2 m. Light was launched into AOTF1 using a fibre collimator (omitted in Fig. 1), which ensured a 1.2-mm beam diameter and beam divergence of at most 0.8 mrad.

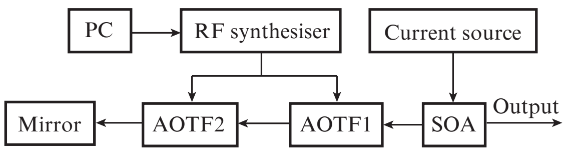

Figure 1. Simplified schematic of the tunable laser.

Both AOTFs had built-in Peltier microcoolers for stabilising the working temperature of the acousto-optic cells. The filters were controlled using the board of an AD9958 two-channel digital frequency synthesiser (Analog Devices). The timing of the channels was performed using one quartz oscillator on an RF synthesiser board, which allowed us to obtain identical phase characteristics of RF signals in the two channels. To reach the desired electric power, the signals from the outputs of the synthesiser board were further amplified by a two-channel power amplifier. The synthesiser was controlled by a personal computer (PC).

The pair of AOTFs used had optimal characteristics for mutual operation. AOTF1 was suitable for both horizontal and vertical light polarisations at its input, whereas AOTF2 required a vertical polarisation vector orientation. To meet this requirement, the polarisation vector at the input of AOTF1 was oriented horizontally, because at its output the polarisation converted into vertical one. The power of the RF signals controlling both filters was 0.1 W.

After each filter insertion and adjustment step in the external cavity scheme, we thoroughly measured the response functions and diffraction efficiencies of the filters. The measurement results are presented in Fig. 2, which demonstrates that the width of the response function of the AOTFs decreases by a factor of 2.4 as a result of two passes through the filters, in agreement with data reported by Voloshinov et al. [8]. The considerable narrowing of the response function is an obvious advantage of the linear external cavity configuration over the ring configuration, in which the width of the response function in the case of two AOTFs can only decrease by a factor of 1.41. The diffraction efficiency of the acousto-optic filters was as high as 92%.

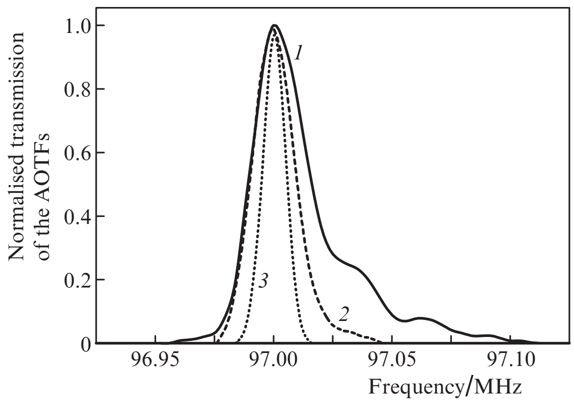

Figure 2. Normalised transmission of the AOTFs as a function of RF control signal frequency: (*1*) at the output of AOTF1, (*2*) at the output of AOTF2 and (*3*) after reflection from the mirror and a second pass through both AOTFs.

3. Steady-state power and spectral characteristics of the laser

Figure 3 shows the light–current curve of the laser under study. The data were obtained at a control signal frequency of 97 MHz for both AOTFs, corresponding to a laser wavelength of 860 nm. The threshold injection current was 28 mA, with a differential quantum efficiency of 0.16 mW mA^{-1}.

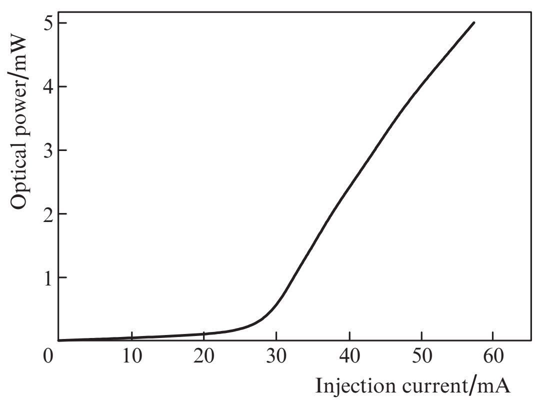

Figure 3. Steady-state light–current curve of the laser tuned to a wavelength of 860 nm.

The laser wavelength was measured as a function of RF control signal frequency for the AOTFs (Fig. 4) at an optical power maintained at a level of 1 mW in order to maximise the wavelength tuning range.

Figure 5 shows the SOA injection current as a function of laser wavelength at two levels of output optical power. The laser wavelength tuning range was 68.7 nm at an output

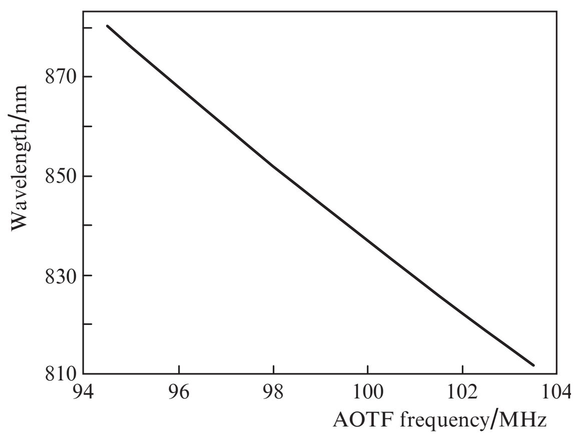

Figure 4. Laser wavelength as a function of AOTF control signal frequency.

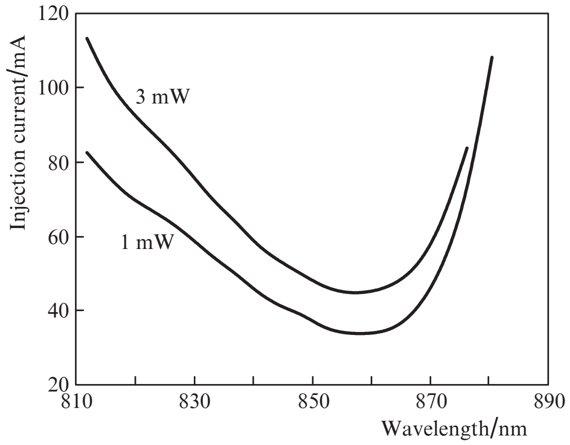

Figure 5. SOA injection current as a function of laser wavelength for spectral tuning with automatic control over the output optical power.

power of 1 mW and 64.4 nm at a power of 3 mW. The maximum injection current at the edges of the tuning range did not exceed 120 mA. The output beam was highly polarised, and the extinction coefficient was near 20 dB.

The emission spectrum of the laser, measured with an Advantest Q8347 optical spectrum analyser, is shown in Fig. 6. The limiting spectral resolution of the Advantest Q8347, 0.003 nm (1.2 GHz), proved insufficient for accurately determining the emission linewidth.

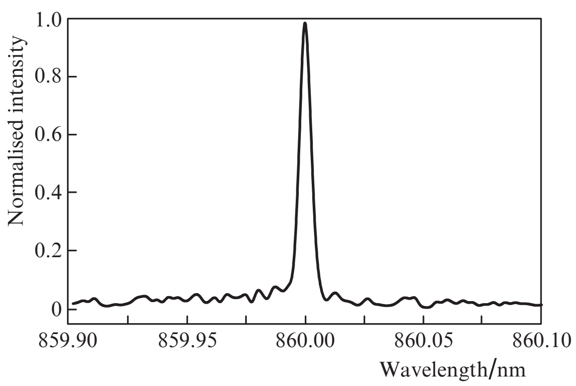

Figure 6. Steady-state emission spectrum of the laser at an AOTF control signal frequency of 97 MHz. The full width at half maximum of the emission line is 0.0056 nm at an output optical power of 3 mW.

In the optical scheme used here, light is outcoupled directly from the active channel of the SOA. As a consequence, the output emission spectrum has a 'superluminescent pedestal'. In this connection, an important parameter of such a laser is the difference between the spectral maximum and the superluminescent background. In the corresponding spectra measured in the range 800–885 nm at an output power of 3 mW (Fig. 7), the difference between the height of the spectral line and the pedestal is ~45 dB (above 30 000) throughout the tuning range.

To obtain accurate data on the emission linewidth, we used a scanning confocal nearest-IR Fabry–Perot interferometer with a free spectral range of 1.5 GHz and optical

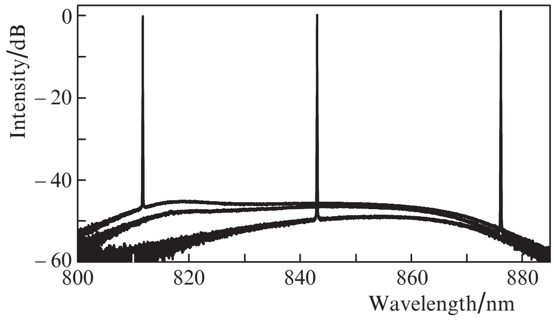

Figure 7. Output emission spectra of the laser at an output power of 3 mW and different positions of the emission line.

resolution of 7.5 MHz. The measurement system is schematised in Fig. 8. To preclude the effect of back-reflected light on the performance of the laser, an optical isolator with >30 dB isolation was placed at the input of the measurement system. The laser beam was focused into the interferometer by a plano-convex lens, which ensured the desired beam waist diameter in the interferometer cavity. The electronic control unit scanned the interferometer mirror, generated signals for synchronisation of the spectrum on the display of the oscilloscope and had a built-in transimpedance amplifier for amplifying the signal from the output photodiode of the interferometer. As an illustration, Fig. 9 shows spectra obtained with the scanning Fabry–Perot interferometer.

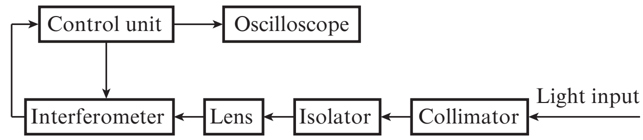

Figure 8. Block diagram of the system used to measure the emission linewidth.

Figure 10 shows the emission linewidth (FWHM), measured with the scanning interferometer, as a function of output optical power. The laser operated in a steady state, and the control signal frequency was 97 MHz for both AOTFs. It is seen from these data that the laser linewidth is a weak function of output power.

It is worth noting that, in the case of steady-state laser operation, we observed unstable behaviour of the spectral line, which showed up as hops to different wavelengths in a range 3–4 GHz wide. The line was often observed to split into two, three or even more components, differing in intensity. The characteristic hop time was a few seconds. It is reasonable to assume that the instability was due to imperfect thermal stabilization of the SOA and AOTFs and the lack of thermal stabilization of the fibre portion of the external cavity. It is worth mentioning here that, at an external cavity length of about 2 m, the longitudinal mode spacing is about 50 MHz. Considerably reducing the external cavity length would be expected to significantly improve the stability of single-frequency lasing, but this will involve serious technological problems.

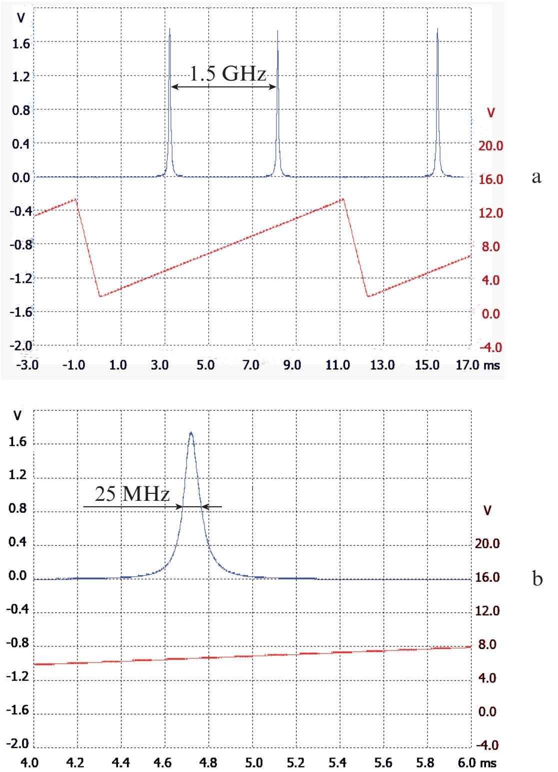

Figure 9. Optical spectra obtained with the scanning Fabry–Perot interferometer: (a) wide-scan spectrum, (b) emission line.

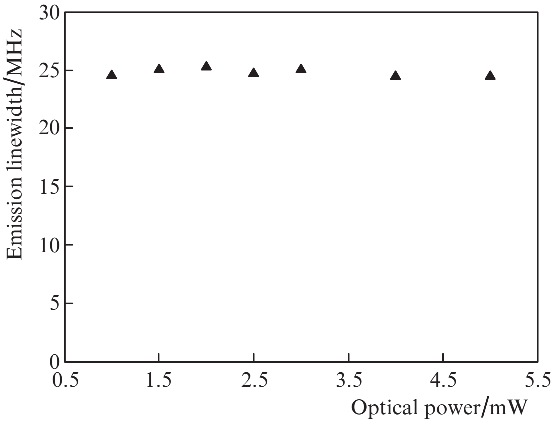

Figure 10. Measured emission linewidth (FWHM) as a function of laser output power.

4. Spectral characteristics of the tunable laser in sweep mode

An important operation mode of a tunable laser is emission wavelength sweeping at a preset rate. In this mode, the laser linewidth can considerably increase with sweep rate. To measure the emission linewidth, we used a monolithic Fabry–Perot etalon for an appropriate spectral range, with a free spectral range of 0.12 nm (48 GHz) and optical resolution of 0.01 nm (4 GHz). Laser light was coupled into the Fabry–Perot etalon using a fibre collimator, which ensured a beam diameter of 3 mm. The light at the output of the etalon was detected by a silicon photodiode with a rise time of 1 ns. The photodiode output was visualised on the display of an oscilloscope. As an example, Fig. 11a shows a spectrum recorded at the etalon output at a tuning rate of 460 nm s^{-1}. Figure 11b shows the output signal of a confocal Fabry–Perot interferometer with a free spectral range of 10 GHz and resolution of 68 MHz, recorded at zero sweep rate, without applying voltage to the interferometer. Comparison of these oscilloscope traces demonstrates that the linewidths obtained are essentially identical.

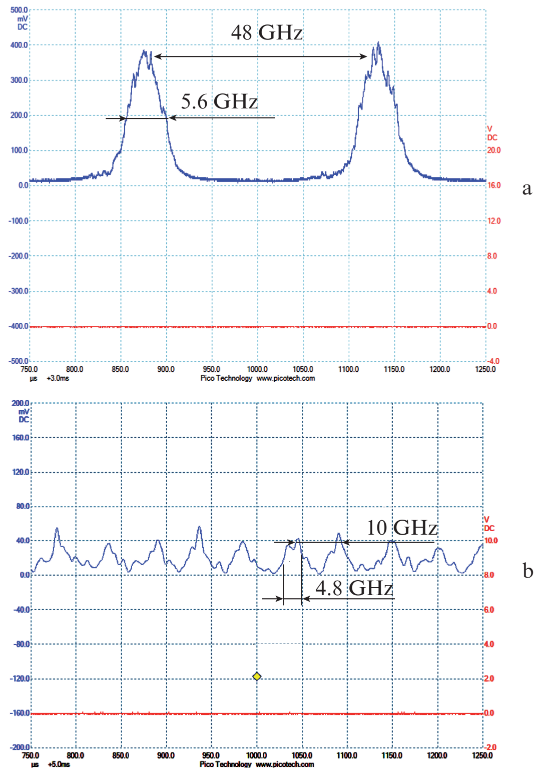

Figure 11. Spectra at the output of a monolithic Fabry–Perot etalon (a) and scanning Fabry–Perot interferometer without wavelength sweeping (b).

Figure 12 shows the laser emission linewidth measured with the monolithic Fabry–Perot etalon as a function of wavelength tuning rate. It is seen that, with increasing tuning rate, the measured instantaneous emission linewidth increases

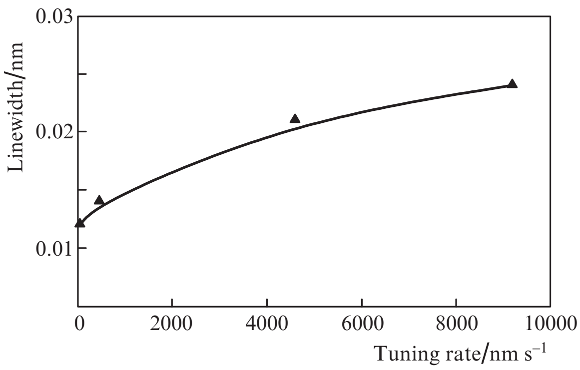

Figure 12. Laser emission linewidth (FWHM) as a function of wavelength tuning rate.

from 0.012 to 0.024 nm. With allowance for the spectral resolution of the interferometer, the true linewidth range is 0.007–0.022 nm. In the case of an external cavity with one acousto-optic filter, typical values of this parameter lie in the range 0.05–0.06 nm. Clearly, there is a substantial benefit due to the Doppler frequency shift compensation in the AOTFs.

Figure 13 shows a time dependence of output power, maintained at a level of 3 mW by an APC system, in the case of periodic laser wavelength sweeping. Its apparent variation is due to the fact that the spectral dependence of sensitivity for the photodiode in the APC system differs from that of the recording photodetector.

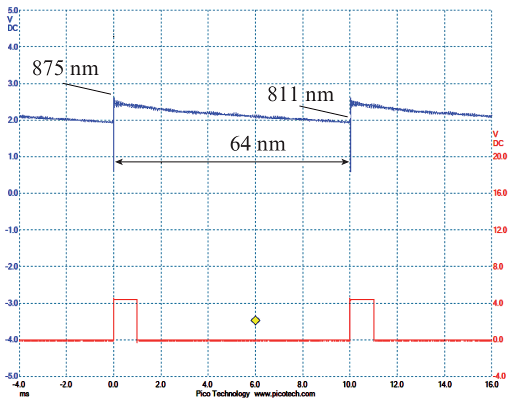

Figure 13. Time dependence of the laser output optical power during periodic wavelength sweeping between 875 and 811 nm at a rate of about 10^4 nm s^{-1}.

5. Conclusions

The present results demonstrate that the use of a semiconductor laser with a linear external cavity containing two AOTFs that ensure Doppler frequency shift compensation allows one to considerably reduce the emission linewidth in both a steady state and sweep mode relative to a laser with a single AOTF, without Doppler shift compensation [9].

In a steady state and at zero mismatch between the AOTF control signal frequencies, the laser linewidth is as small as 25 MHz, which is almost three orders of magnitude smaller than in the case of one filter. At the same time, the position of the emission line is unstable and slowly fluctuates in a range 3–4 GHz wide, without preventing us from obtaining light with a large coherence length.

In sweep mode, the laser emission line is markedly broader, but does not exceed 0.022 nm (8.8 GHz) at the highest wavelength tuning rate for the type of AOTF used: 10^4 nm s^{-1}.

The present experimental data demonstrates the possibility of producing a commercially viable instrument based on a tunable semiconductor injection laser with the following performance parameters: optical power at the SMF output, 3 mW; wavelength tuning range, 815–875 nm; maximum tuning rate, 10^4 nm s^{-1}; instantaneous linewidth during tuning, no greater than 0.025 nm; difference between the spectral maximum and superluminescent background, at least 40 dB; steady-state coherence length, at least 10 m; extinction coefficient at the SMF output, at least 17 dB.

The length of the external laser cavity can be reduced to 200–250 mm, which is expected to further reduce the output linewidth and improve the stability of the emission spectrum. The output optical power can be considerably raised by using a spectrally matched travelling-wave SOA at the laser output.

References

1. Duarte F.J. *Tunable Lasers Handbook* (New-York: Academic Press, 1995).
2. Coquin G.A., Cheung K.W. *Electron. Lett.*, **24** (10), 599 (1988).
3. Coquin G.A., Cheung K.W. *IEEE J. Quantum Electron.*, **25** (6), 1576 (1989).
4. Ward J.D., Pannell C.N. *Phys. Procedia*, **70**, 914 (2015).
5. Chamorovsky A.Yu., Lobintsov A.A., Shramenko M.V., Yakubovich S.D. *Proc. SPIE*, **9697**, 96972T-1 (2016).
6. Mamedov D.S., Marmalyuk A.A., Prokhorov V.V., Yakubovich S.D. *Quantum Electron.*, **34** (3), 206 (2004) [*Kvantovaya Elektron.*, **34** (3), 206 (2004)].
7. Andreeva E.V., Il'chenko S.N., Ladugin M.A., Lobintsov A.A., Marmalyuk A.A., Shramenko M.V., Yakubovich S.D. *Quantum Electron.*, **43** (11), 994 (2013) [*Kvantovaya Elektron.*, **43** (11), 994 (2013)].
8. Voloshinov V.B., Magdich L.N., Knyazev G.A. *Quantum Electron.*, **35** (11), 1057 (2005) [*Kvantovaya Elektron.*, **35** (11), 1057 (2005)].
9. Andreeva E.V., Magdich L.N., Mamedov D.S., Ruenkov A.A., Shramenko M.V., Yakubovich S.D. *Quantum Electron.*, **36** (4), 324 (2006) [*Kvantovaya Elektron.*, **36** (4), 324 (2006)].